

11.3 ASSESSING THE UTILITY OF TOTAL LIGHTNING AND THE LIGHTNING JUMP TO ASSIST IN THE QLCS TORNADO WARNING DECISION PROCESS

Brett M. Williams* and Lawrence D. Carey
Department of Atmospheric Science
University of Alabama in Huntsville, Huntsville, Alabama

1. INTRODUCTION AND BACKGROUND

Quasi-linear convective systems (QLCS) are organized lines of convection that commonly occur over portions of the United States (Trapp et al. 2005), and can produce all forms of severe weather, including hail, strong straight-line winds, and occasionally can spawn tornadoes (Smith et al. 2012). Trapp et al. (2005) found that about 18% of all tornadoes in the US are associated with QLCSs. Tornadoes associated with QLCSs differ in many ways from supercells. They form in different convective environments, take on completely different appearances on radar and have different microphysical and dynamical processes. QLCS tornadoes do not typically produce a descending velocity signature on radar, which is an important precursor for supercell tornadoes. Instead, they usually produce mesovortices, which typically exist within a few km of the surface, tend to quickly build upward, and possess compact couplets (Houze 2004). These features can make it very difficult to identify mesovortices on radar, especially if the QLCS of interest is at a great distance from a WSR-88D radar, in which the rotation may be below the lowest elevation angle. Furthermore, there is the threat for tornadoes to form in many locations along the QLCS convective line, as opposed to only one area favored for tornadogenesis within a supercell (Newman and Heinselman 2012). Due to all of these factors, NWS performance on QLCSs is significantly worse compared to supercells. Brotzge et al. (2013) shows that the prominent skill score metrics of probability of detection (POD) and lead time are significantly worse for QLCSs compared to supercells. This can be seen in Figure 1. The POD and lead time for QLCS tornadoes vs. a discrete right-mover supercell tornado was ~50% and ~13 minutes vs. ~90% and ~18 minutes. Additionally, a study of all tornado

warnings issued by the NWS in Huntsville, AL since October 2007, seen in Figure 2, yielded significantly poorer skills scores of false-alarm ratio (FAR), POD, and critical score index (CSI) for QLCS tornadoes compared to supercell tornadoes, with POD being the most significant (38% for QLCS vs 68% for supercell). Thus, it is clear that any additional information that a warning forecaster could gather from total lightning information that could hint to the increased likelihood of QLCS tornadogenesis has the potential to be highly valuable.

With the launching of GOES-R in the near future and the implementation of the Geostationary Lightning Mapper (GLM), NWS forecast offices will have access to high resolution, both temporal and spatial, lightning information. Several studies in the past have correlated increases in total flash rate within a storm to severe weather occurrence (Schultz et al. 2009, 2011, Williams et al. 1999, Gatlin and Goodman 2010). A rapid increase in total lightning is termed a lightning jump, and indicates a significant intensification of updraft strength (Schultz et al. 2015, in revision). An example of a lightning jump can be seen in Figure 3. Lightning jumps can be used to increase situational awareness and perhaps tip-the-scales in the warning decision process. However, lightning jumps are used as a proxy for general severe weather occurrence and do not necessarily discriminate between types of severe weather (e.g. tornadoes, hail, and wind). However, potential connections exist between total lightning and mesovortex formation, which is the parent circulation from which QLCS tornadoes are born. Many studies have found that mesovortexgenesis is initiated at low levels by tilting, in downdrafts, of crosswise baroclinic horizontal vorticity (Trapp and Weisman 2003 Part II, Wheatley and Trapp 2008, Atkins and St. Laurent 2009 Part II). A schematic of this process can be seen in Figure 4. Additional studies have found that strong low-level updraft is critical in converging and amplifying vertical vorticity associated with the mesovortex (Schenkman et al. 2012, Atkins and St. Laurent 2009). A four-step schematic which includes the

* Corresponding author address: Brett M. Williams, Univ. of Alabama in Huntsville – Atmospheric Science, National Space Science and Technology Center, 320 Sparkman Dr., Huntsville, AL 35805. Email: bw0026@uah.edu

role of a strong low-level updraft in mesovortex formation can be seen in Figure 5. Lightning is related to both updraft and downdraft strength. A lightning jump is an indication of an increase in updraft strength (Schultz et al. 2015). Larger flash rates correlate to a more intense updraft. A stronger mid-level updraft helps electrify the storm and produce more, larger ice precipitation which can lead to a stronger downdraft by more precipitation loading and melting. Thus, it is feasible that a stronger updraft and downdraft, indicated by an increase in total flash rate, within an environment with strong ambient low-level wind shear, could perhaps suggest that specific region of the QLCS is more favored for mesovortex formation. The ultimate objective of this research is to assess if total lightning and the lightning jump be used by NWS warning forecasters as an additional tool that can be used to improve operation on QLCS events.

2. METHODOLOGY

All four analyzed QLCS cases were selected from within the domain of the Huntsville, AL National Weather Service (NWS) County Warning Area (CWA) and the North Alabama Lightning Mapping Array (NALMA). Two cases were categorized as a tornadic QLCS and two cases were categorized as a non-tornadic QLCS. The two non-tornadic QLCS cases had multiple tornado warnings issued on the QLCS over its lifetime. The four cases are as follows: a) 21 February 2014 tornadic QLCS b) 4 April 2011 non-tornadic QLCS c) 27 April 2011 tornadic QLCS and d) 2 September 2012 non-tornadic QLCS.

A thorough analysis was performed, both qualitative and quantitative, between the tornadic and non-tornadic QLCS cases. First, a visual analysis of the characteristics and evolution of the lightning and radar information using WDSS-II was performed (Lakshmanan et al. 2007). This included an interrogation of base reflectivity and 2-minute composite of flash extent density (FED), which is a count of the total number of flashes that traveled through a particular grid point. Then, time series plots of various parameters were plotted from the tracked cells of interest. For the tornadic QLCS cases, these plots included total flash rate, time of a lightning jump, maximum 0-3 km azimuthal shear, and tornado duration(s). For the non-tornadic QLCS cases, these plots included total flash rate, time of a lightning jump, maximum 0-3 km azimuthal shear, tornado warning duration(s) and time of severe wind report(s).

Additionally, assorted near-storm environment parameters were collected from the Storm Prediction Center (SPC) Mesoanalysis archive as well as NWS observed soundings to add context. Environmental parameters for each case can be found in Table 1.

Archived level-II radar data from KHTX, the WSR-88D radar in Hytop, AL, was obtained from the NCDC archive and processed for visualization in WDSS-II. NALMA lightning information was obtained from an archive maintained and operated by NASA SPoRT at the Marshall Space Flight Center and was also processed for visualization in WDSS-II. 0-3 km azimuthal shear was derived from the Doppler radial velocity using WDSS-II, and is a measure of rotation. This was used as a proxy for the presence and strength of a mesovortex.

Table 1 – Assorted wind shear and instability parameters for all four cases

Parameter	21 Feb 2014	4 Apr 2011	27 Apr 2011	2 Sept 2012
0-1 km Bulk Shear [kts]	40	40	55	10
Effective Shear [kts]	60	50	70	20
BRN Shear [$\text{m}^2 \text{s}^{-2}$]	80	120	200	30
MU CAPE [J kg^{-1}]	750	750	750	2750

To make the time series plots of the tracked cells of interest, some sort of consistent tracking methodology had to be employed. This process was very challenging due to the difficulty in identifying the individual cell from within the QLCS convective line as a whole that was pertinent to the analysis in each case. First, tracking by reflectivity was attempted. This was not very successful, as it usually tracked either too large or too small of an area. Tracking by flash extent density worked appreciably better. Ultimately, a hybrid tracking methodology was employed, using both objective and subjective tracking methods. Tracking by flash extent density was employed using the WDSS-II command w2segmotionll. The latitude and longitude coordinates of the center point of the tracked cell by flash extent density that corresponded to the region of the QLCS that was associated with the tornadoes (tornado warnings) were used as the center point of the tracking area.

To create the tracking region, a box 30 km in latitude by 30 km in longitude was employed for a total area of 900 km². This tracking box was chosen because it is large enough to be a sizable area but still small enough to highlight the specific region of interest along the QLCS convective line. Additionally, the average tornado warning polygon area for all tornado events within the Huntsville CWA from October 2007 to January 2015 was 911 km². Since flash extent density was available every two minutes, a tracking area “box” was created every two minutes. Every case analyzed possessed this total tracked area of 900 km². This was done to keep tracking area consistent for each case, as total flash rate is a counting stat of all flashes within the tracked area, and differences in size of tracked area could skew results. Total flash rate is a measure of the total number of lightning flashes that occurred within that 900 km² box. Maximum 0-3 km azimuthal shear was computed by finding the maximum value of 0-3 km azimuthal shear within the tracked 900 km² box at each new radar volume scan. These values were retrieved using `w2polygon2csv` in `WDSS-II`, which can find the maximum value of any variable within a user-given polygon. These values were then confirmed by hand. While tedious, this was done to ensure that the values were correct, as 0-3 km azimuthal shear tends to be a bit noisy and it is not uncommon for an artificial large positive value to occur that is not associated with any actual rotation.

The 2-sigma lightning jump algorithm was utilized for this study (Schultz et al. 2009; 2011). The LMA source data was clustered into individual flashes using a spatial and temporal clustering algorithm developed by McCaul et al. (2005). Flashes were thresholded at ten sources or greater to filter out smaller lightning flashes (Wiens et al. 2005). Since the flash data is every two minutes, a one minute flash rate was created averaging out the two minute flash data. From there, the time rate of change of the total flash rate was calculated, denoted by `DFRDT` or derivative of flash rate over derivative of time. A standard deviation (σ) was calculated from the most recent five periods of `DFRDT`, not including the current observation time. A lightning jump occurs when the current `DFRDT` $\geq 2*\sigma$ and the current flash rate ≥ 10 flashes min⁻¹. This flash rate threshold was implemented to filter out insignificant lightning jumps.

3. RESULTS

a) CASE #1: 21 FEBRUARY 2014 TORNADIC QLCS

This case was characterized by strong wind shear and weak instability. The tornadoes produced by this particular QLCS occurred in two distinct clusters. Cluster 1 occurred between 0245 and 0315 UTC, producing 4 EF-1 tornadoes. Cluster 2 occurred between 0353 and 0430 UTC and produced 3 EF-1 tornadoes. Only one of these seven tornadoes had an accompanying tornado warning issued, thus resulting in six missed tornadoes. As can be seen in Figure 6, the tornadoes from cluster 1 were associated with the region of the QLCS that was associated with the most intense flash rates. Cluster 2 tornadoes were associated with lower flash rates than cluster 1, relatively speaking, but were still associated with the area of most intense flash rates at that time (Figure 6). Additionally, bowing segments as well as appendages in reflectivity were observed at the locations of both tornado clusters, and these features were co-located with the maximum flash rates along the QLCS convective line, which can be seen in Figure 7.

From the time series (Figure 8), the maximum flash rate over the observed period was 72 flashes min⁻¹ with a mean flash rate of 26.9 flashes min⁻¹. Two lightning jumps preceded the first tornado of Cluster 1 with a lead time of 21 and 7 minutes, respectively, and a lightning jump preceded the first tornado of Cluster 2 with a lead time of 29 minutes. The flash rate remained above 50 flashes min⁻¹ for the duration of the first tornadic period, and the flash rate then decreased after the 0324 UTC lightning jump and were relatively low (< 20 flashes min⁻¹) for the duration of the second tornadic period. The lightning jumps preceded an increase in maximum 0-3 km azimuthal shear that reached its peak in conjunction with the first tornadic period. A local maximum in the flash rate occurred around 0342 UTC that preceded the second increase in maximum 0-3 km azimuthal shear that coincided with the second tornadic period. Thus, in both cases, a lightning increase did occur prior to an azimuthal shear increase and tornadogenesis, although it is more obvious with the Cluster 1 tornadoes.

b) CASE #2: 4 APRIL 2011 NON-TORNADIC QLCS

This case had a very similar near-storm environment to the above tornadic QLCS case from 21 February 2014. It was characterized by

strong wind shear and weak instability. This particular case had three tornado warnings issued on it, all of which resulted in a false alarm. The flash rate reaches maximum intensity around 2008 UTC co-located very closely with the 2003 UTC tornado warning issued in southern Tennessee, seen in Figure 9. There are no obvious bowing structures or appendages/hooks present in the reflectivity field that would suggest an ongoing or incipient tornado. The time series (Figure 10) from this case was from the tracked cell that was associated with the two tornado warnings at 2003 UTC and 2029 UTC in southern Tennessee. The maximum flash rate over the observed period was 22 flashes min^{-1} with a mean flash rate of 8.8 flashes min^{-1} . Two lightning jumps occurred at 1939 and 1957 UTC that preceded the issuance of first tornado warning. There were multiple severe wind reports associated with local maxima in flash rate and another associated with secondary peak in 0-3 km azimuthal shear around 2042 UTC. The maximum 0-3 km azimuthal shear roughly followed the trend of the flash rate and peaked about ten minutes after the second lightning jump. The first jump was not associated with an increase in maximum 0-3 km azimuthal shear while the second jump preceded a small increase in maximum 0-3 km azimuthal shear.

c) CASE #3: 27 APRIL 2011 TORNADIC QLCS

The second tornadic QLCS case analyzed comes from the famous April 27, 2011 super-outbreak across the southern United States. This was the midday QLCS that came after the early morning tornadic QLCS and before the supercell event of the afternoon and evening (Knupp et al. 2014). This case was characterized by very strong wind shear and relatively weak instability. A total of seven tornadoes were produced by this QLCS between 1615 UTC and 1705 UTC. Four of these tornadoes were rated EF-1, including a 21-mile long tornado, and three were rated EF-0. Similarly to the 21 February 2014 tornadic QLCS case, all tornadoes were associated with the region of the QLCS that had the most intense flash rates (Figure 11). Furthermore, numerous appendages and hooks in the reflectivity associated with the tornadoes were co-located with the maximum flash rate along the QLCS convective line at that time (Figure 11).

From the time series plot in Figure 12, the flash rate peaked at 45 flashes min^{-1} at 1646 UTC with an average flash rate of ~ 27 flashes min^{-1} for the duration of the tornadic period. Two lightning

jumps preceded the first tornado by 37 and 21 minutes, respectively, with an additional lightning jump observed at 1645 UTC, during the tornadic period. Maximum 0-3 km azimuthal shear displayed an overall increasing trend, peaking near 0.02 sec^{-1} at 1702 UTC, concurrent with a long-track EF-1 tornado. All lightning jumps preceded an increase in maximum 0-3 km azimuthal shear for this case.

d) CASE #4: 2 SEPT 2012 NON-TORNADIC QLCS

This particular case had a very different environment compared to the other three cases in this study. This case was characterized by weak wind shear and very strong instability. A total of nine tornado warnings were issued this day by the Huntsville WFO, all of which resulted in false alarms. Figure 13 shows multiple areas of intense flash rates along the QLCS convective line over its life-cycle, but only one bowing segment present and no appendages or hooks present in the reflectivity field.

Figure 14 depicts the time series plot for this particular case that was associated with five tornado warnings issued over a period of three hours as the QLCS traversed from NW Alabama to NE Alabama. The maximum flash rate during the period was 43 flashes min^{-1} with a mean flash rate of 15.5 flashes min^{-1} . Flash rates had a pulsing pattern, where they would increase, reach maxima, decrease, and then repeat. There were four lightning jumps present, which occurred at start of each pulse following the decrease in flash rate from the preceding pulse. Severe wind reports were associated with the local maxima in flash rate except for the report at ~ 2350 UTC, which was associated with a maximum in 0-3 km azimuthal shear. Maximum 0-3 km azimuthal shear increased slightly following each jump and increased gradually throughout the entire period, but to a lesser extent than the two tornadic cases.

4. SUMMARY

The following list is a summary of the key trends and observations from the analysis of the four QLCS cases in this study:

- 1) All four cases had multiple lightning jumps present. Additionally, all lightning jumps preceded severe weather occurrence (tornadoes and/or severe wind).

2) Tornadoic cases had larger flash rates than non-tornadoic cases, both in peak flash rate as well as average flash rate. The 2 September 2012 non-tornadoic case which was characterized by greater flash rates was also characterized by very low wind shear, which likely played a large role in why it did not produce tornadoes.

3) Tornadoes from both tornadoic cases were associated with the region of the QLCS with the most intense flash rates at that time.

4) A large percentage of lightning jumps and increases in flash rate preceded an increase in maximum 0-3 km azimuthal shear. Furthermore, the two tornadoic cases displayed greater azimuthal shear values than non-tornadoic cases as well as a greater propensity for azimuthal shear to increase following a lightning jump.

5) Tornadoic cases were characterized by numerous bowing segments, inflow notches, and appendages or hooks along the convective line. Lightning jumps preceded the formation of these features and these features were also co-located with the area of largest flash rates along the QLCS convective line at that time. The two non-tornadoic cases had an overall less prevalence of these features.

5. CONCLUSIONS

These results suggest that lightning information and the lightning jump could indeed be useful in the QLCS tornado warning decision process. Of course, these results are preliminary, as only four cases have been analyzed thus far. There are many more cases left to interrogate. However, these four cases support the following hypothesis:

1) Lightning jumps and/or very intense flash rates associated with a specific segment of the QLCS has the potential to indicate to a forecaster that particular area is most favorable for mesovortexgenesis, even before traditional radar methods can indicate this from the formation of a bowing segment, hooks or appendages in reflectivity, or a velocity couplet, thereby increasing forecaster situational awareness.

2) When radar and environmental conditions suggest the potential for a QLCS tornado, utilizing total lightning information and the lightning jump can be an additional piece of information that can tip the scales for a forecaster in the tornado warning decision process.

Additional case studies will provide evidence that either further supports or contradicts these hypotheses.

Other applications of this work include potentially improving warnings for significant QLCS straight line wind events. Future work will include analyzing more cases. Additionally, dual-Doppler analysis on select cases for 3D wind field retrieval will be performed, as well as an analysis of QLCS cases with no associated severe weather of any kind to observe how the lightning behaves in those cases. Lastly, an examination of QLCS cases from other regions, such as the Oklahoma Lightning Mapping Array (OKLMA), the Colorado Lightning Mapping Array (COLMA), the West Texas Lightning Mapping Array (WTLMA) and the D.C. Lightning Mapping Array (DCLMA) will be performed for comparison with the results from the NALMA.

Acknowledgements. This research has been supported by the NOAA GOES-R Risk Reduction Research (R3) program. In particular, the authors would like to thank Dr. Steven Goodman, Senior (Chief) Scientist, GOES-R Program for his guidance and support throughout this effort. Also, the authors would also like to thank Chris Schultz and Sarah Stough for their assistance.

6. REFERENCES

- Atkins, N. T. and M. St. Laurent, 2009: Bow Echo Mesovortices. Part II: Their Genesis. *Mon. Wea. Rev.*, **137**, 1514–1532.
- Brotzge, J., S. E. Nelson, R. L. Thompson, and B. T. Smith, 2013: Tornado probability of detection and lead time as a function of convective mode and environmental parameters. *Wea. Forecasting*, **28**, 1261-1276.
- Gatlin, P. N., and S. J. Goodman, 2010: A Total Lightning Trending Algorithm to Identify Severe Thunderstorms. *J. Atmos. Oceanic Technol.*, **27**, 3–22.
- Houze, R. A., Jr.: Mesoscale convective systems, *Rev. Geophys.*, **42**, RG4003.
- Knupp, K. R., T. A. Murphy, T. A. Coleman, R. A. Wade, S. A. Mullins, C. J. Schultz, E. V. Schultz, L. D. Carey, A. Sherrer, E. W. McCaul Jr., B. Carcione, S. Latimer, A. Kula,

- K. Laws, P. T. Marsh, and K. Klockow, 2014: Meteorological Overview of the Devastating 27 April 2011 Tornado Outbreak. *Bull. Amer. Meteor. Soc.*, **95**, 1041–1062.
- Lakshmanan, V., T. Smith, G. Stumpf, and K. Hondl, 2007: The Warning Decision Support System – Integrated Information. *Wea. Forecasting*, **22**, 596-612.
- McCaul, E. W., J. Bailey, S. J. Goodman, R. Blakeslee, and D. E. Buechler, 2005: A ash clustering algorithm for North Alabama Lightning Mapping Array data. *Preprints, Conf. on Meteorological Applications of Lightning Data*, San Diego, CA, Amer. Meteor. Soc., CD-ROM, 5.2.
- Newman, J.F., and P.L. Heinselman, 2012: Evolution of a Quasi-Linear Convective System Sampled by Phased Array Radar. *Mon. Wea. Rev.*, **140:11**, 3467-3486.
- Schenkman, A., M. Xue, and A. Shapiro, 2012: Tornadogenesis in a simulated mesovortex within a mesoscale convective system. *J. Atmos. Sci.*, **69**, 3372–3390.
- Schultz, C. J., W. A. Petersen, and L. D. Carey, 2009: Preliminary development and evaluation of lightning jump algorithms for the real-time detection of severe weather. *J. Appl. Meteor. Climatol.*, **48**, 2543-2563.
- Schultz, C. J., W. A. Petersen, and L. D. Carey, 2011: Lightning and severe weather: A comparison between total and cloud-to-ground lightning trends. *Wea. Forecasting*, **26**, 744-755.
- Schultz, C. J., L. D. Carey, E. V. Schultz and R. J. Blakeslee, 2015: Insight into the physical and dynamical processes that control rapid increases in total lightning. *Wea. Forecasting*, in revision.
- Smith, B.T., R.L. Thompson, J.S. Grams, C. Broyles and H.E. Brooks, 2012: Convective modes for significant severe thunderstorms in the contiguous United States. Part I: Storm classification and climatology. *Wea. Forecasting*, **27**, 1114-1135
- Trapp, R. J., and M.L. Weisman, 2003: Low-level vortices within squall line and Bow Echoes: Part II. Their genesis and implications. *Monthly Weather Review*, **131**, 2804-2823.
- Trapp, R. J., S. A. Tessendorf, E. S. Godfrey, and H. E. Brooks, 2005: Tornadoes from squall lines and bow echoes. Part I: Climatological distribution. *Wea. Forecasting*, **20**, 23–34.
- Wheatley, D. M., and R. J. Trapp, 2008: The Effect of Mesoscale Heterogeneity on the Genesis and Structure of Mesovortices within Quasi-Linear Convective Systems. *Mon. Wea. Rev.*, **136**, 4220–4241.
- Wiens, K. C., S. A. Rutledge, and S. A. Tessendorf, 2005: The 29 June 2000 supercell observed during steps. Part II: Lightning and charge structure. *J. Atmos. Sci.*, **62**, 4151-4177.
- Williams, E. R., and Coauthors, 1999: The behavior of total lightning activity in severe Florida thunderstorms. *Atmos. Res.*, **51**, 245-265.

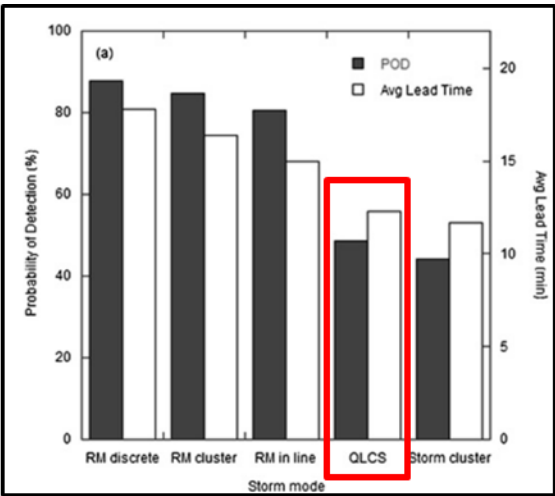


Figure 1: Tornado POD and average lead time for various storm morphologies from all nationwide tornadic events from 2003 to 2004 from Brotzge et al. (2013).

Huntsville WFO

Statistic	QLCS	Supercell
Warnings	141	259
Hits	29	79
Misses	47	37
False Alarms	112	180
Skill Score	QLCS	Supercell
FAR	79.4%	69.5%
POD	38.2%	68.1%
CSI	15.4%	26.7%

Figure 2: Statistics and skill scores for all QLCS and supercell tornado events within the Huntsville (HUN) CWA from October 2007 - September 2014.

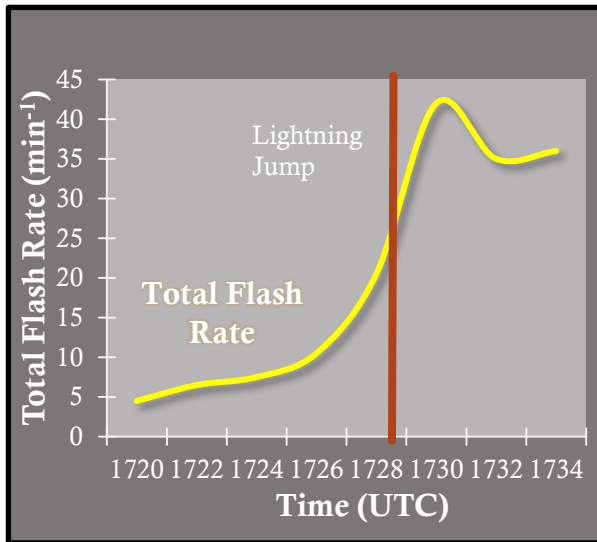


Figure 3: Idealized example of a lightning jump from Schultz et al. (2014).

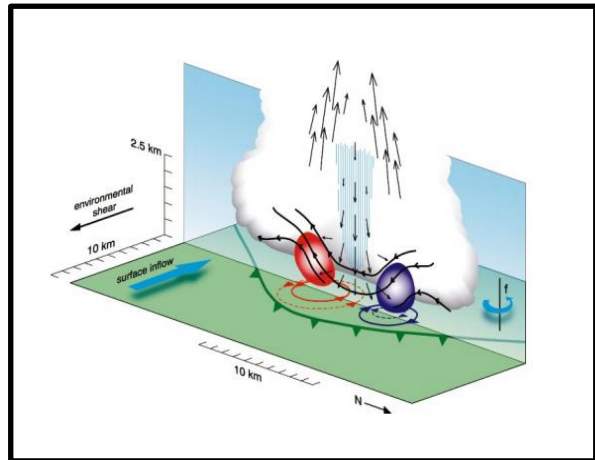


Figure 4: Schematic of tilting of vorticity by downdraft from Trapp and Weisman (2003).

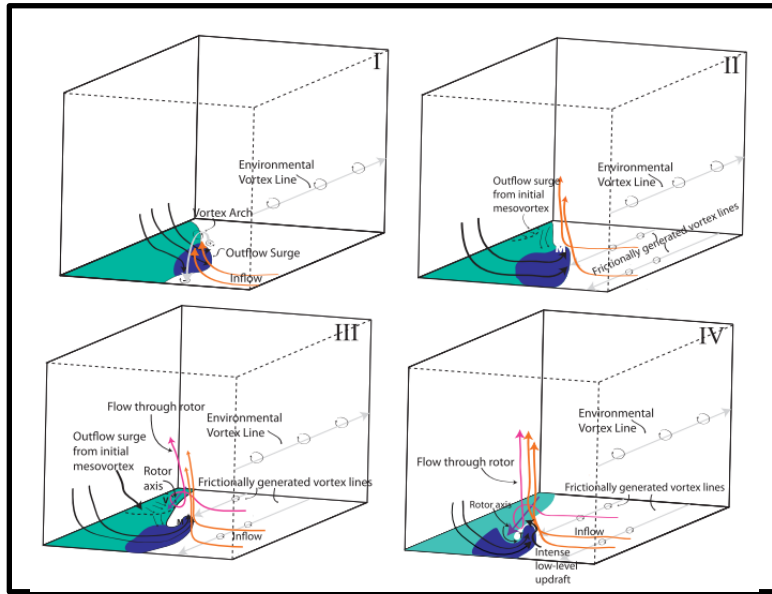


Figure 5: 4-stage conceptual model for tornadogenesis from a mesovortex from Schenkman et al. 2012

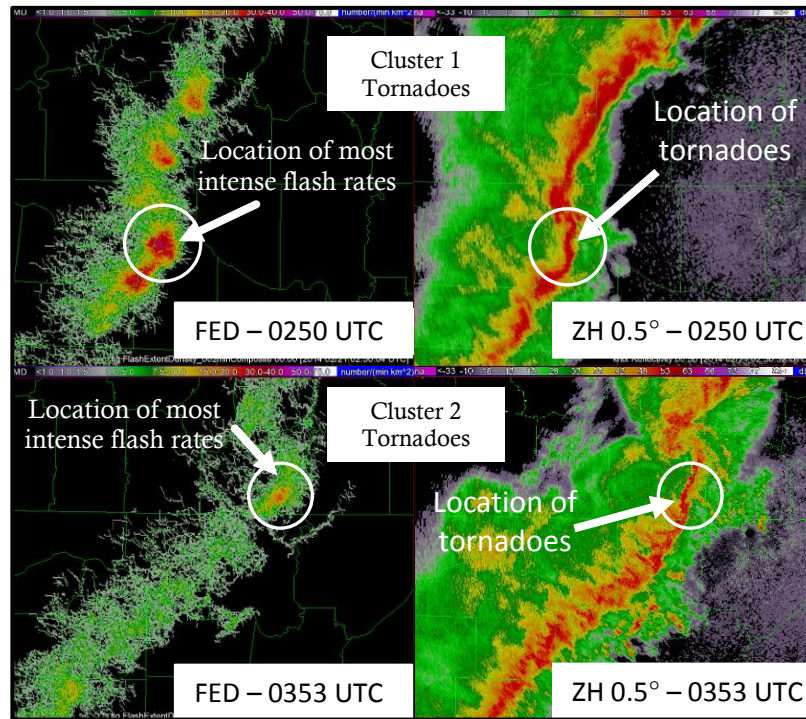


Figure 6: Left: Flash extent density flashes $\text{min}^{-1} \text{km}^{-2}$] (left) and KHTX base reflectivity [dBZ] (right) at 0250 UTC (top) and 0353 UTC (bottom) on 21 February 2014. These times represent the start of each tornadic period.

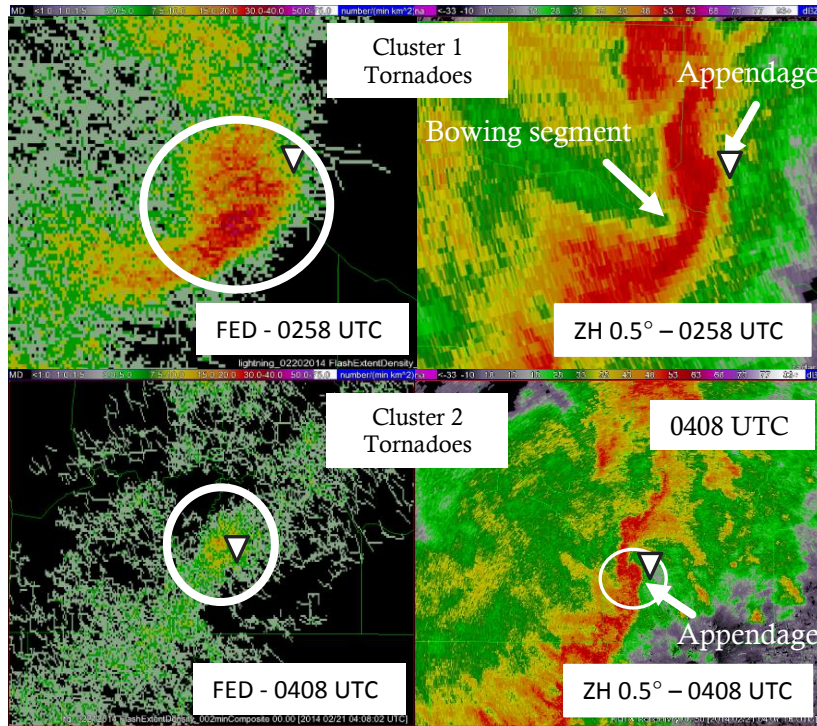


Figure 7: Flash extent density [flashes $\text{min}^{-1} \text{km}^{-2}$] (left) and KHTX base reflectivity [dBZ] (right) at 0258 UTC (top) and 0408 UTC (bottom) on 21 February 2014. Triangle denotes location of tornado.

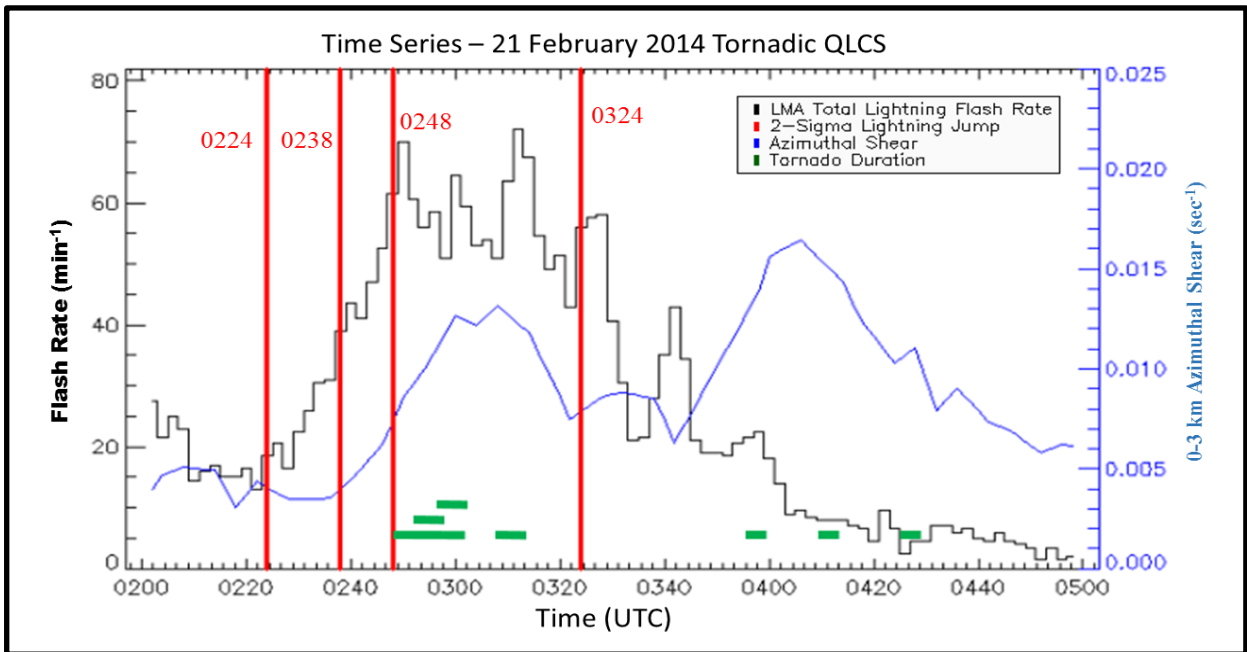


Figure 8: Time series of flash rate [min^{-1}], time of lightning jump, maximum 0-3 km azimuthal shear [sec^{-1}] and tornado durations from tracked cell from 0200 UTC to 0500 UTC on 21 February 2014

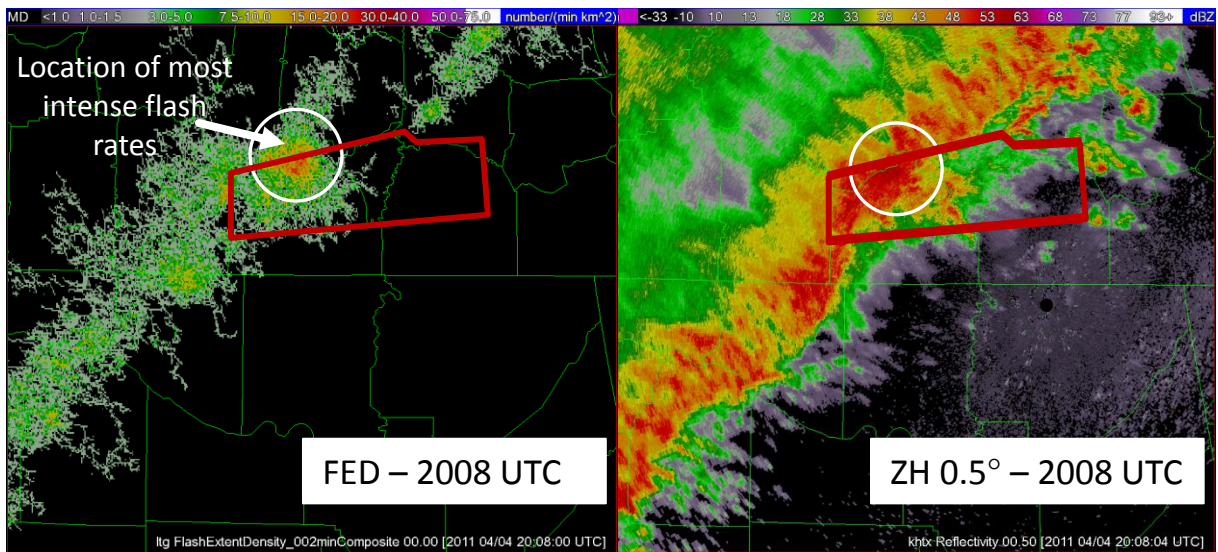


Figure 9: Flash extent density [flashes $\text{min}^{-1} \text{km}^{-2}$] (left) and KHTX base reflectivity [dBZ] (right) at 2008 UTC on 4 April 2011. Red polygon is tornado warning issued at 2003 UTC

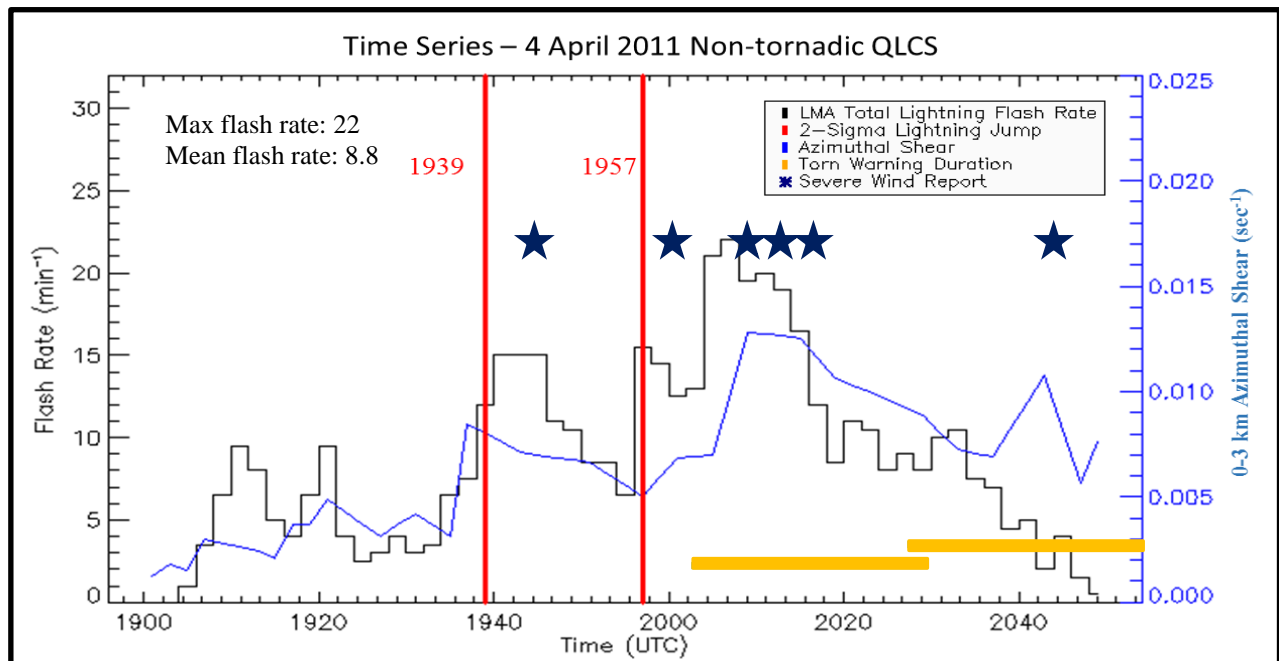


Figure 10: Time series of flash rate [min^{-1}], time of lightning jump, maximum 0-3 km azimuthal shear [sec^{-1}], tornado warning duration and severe wind reports from tracked cell from 1900 UTC to 2059 UTC on 4 April 2011

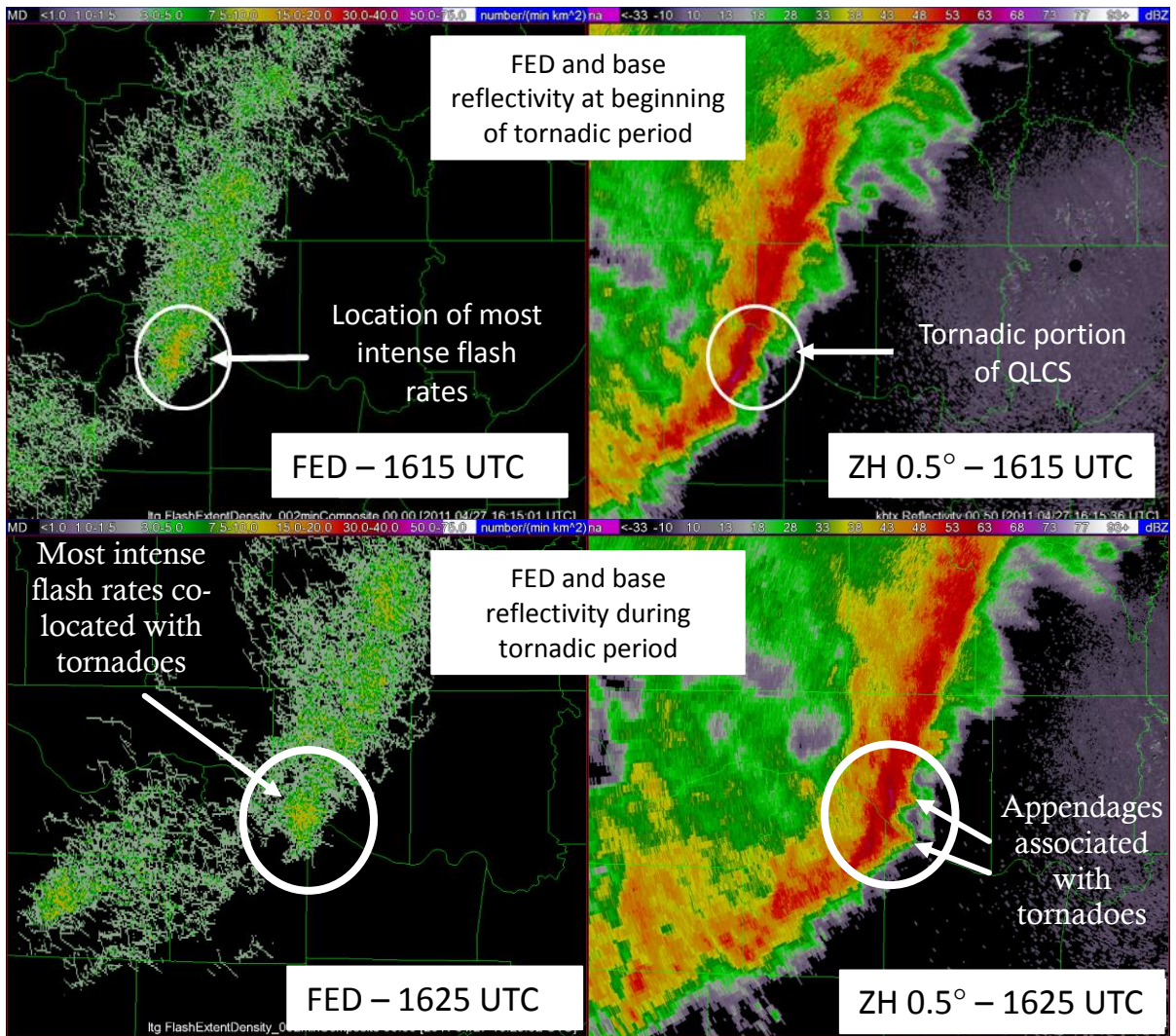


Figure 11: Top: Flash extent density [flashes $\text{min}^{-1} \text{km}^{-2}$] (left) and KHTX base reflectivity [dBZ] (right) at 1615 UTC on 27 April 2011. Note area of most intense flash rates circled in white co-located with tornadic region of QLCS. Bottom: Flash extent density [flashes $\text{min}^{-1} \text{km}^{-2}$] (left) and KHTX base reflectivity [dBZ] (right) for a tornadic QLCS on 27 April 2011 at 1625 UTC

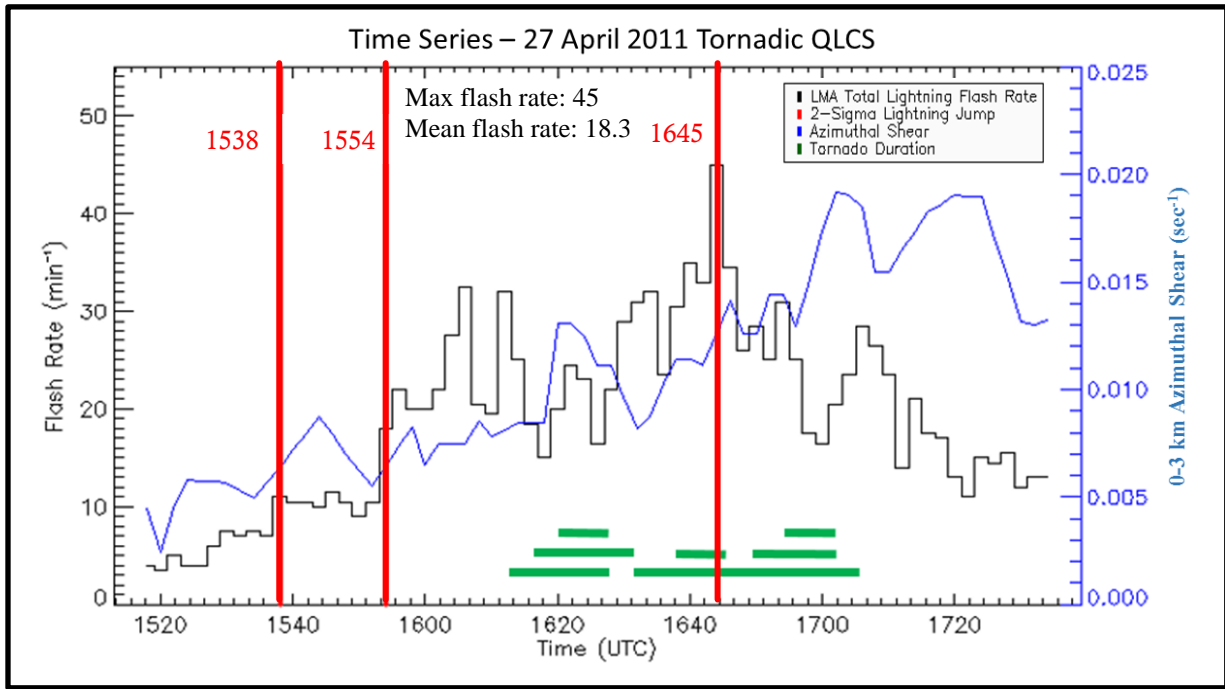


Figure 12: Time series of total flash rate [min^{-1}], time of lightning jump, maximum 0-3 km azimuthal shear [sec^{-1}] and tornado duration from a tracked cell from 1520 UTC to 1745 UTC on 27 April 2011

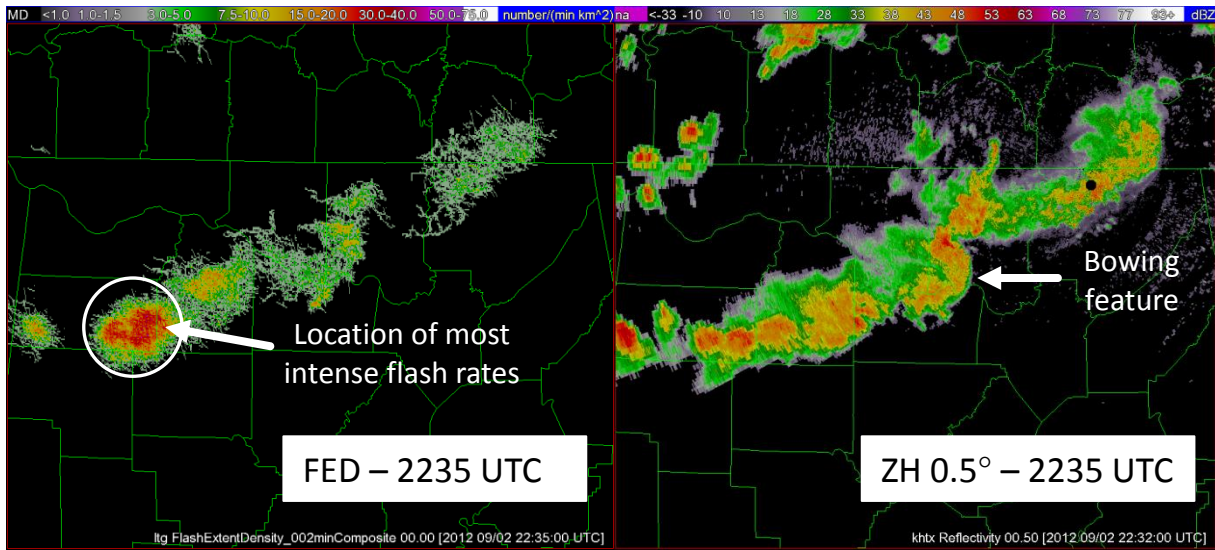


Figure 13: Flash extent density [$\text{min}^{-1}\text{km}^{-2}$] (left) and KHTX base reflectivity [dBZ] (right) at 2235 UTC on 2 September 2012.

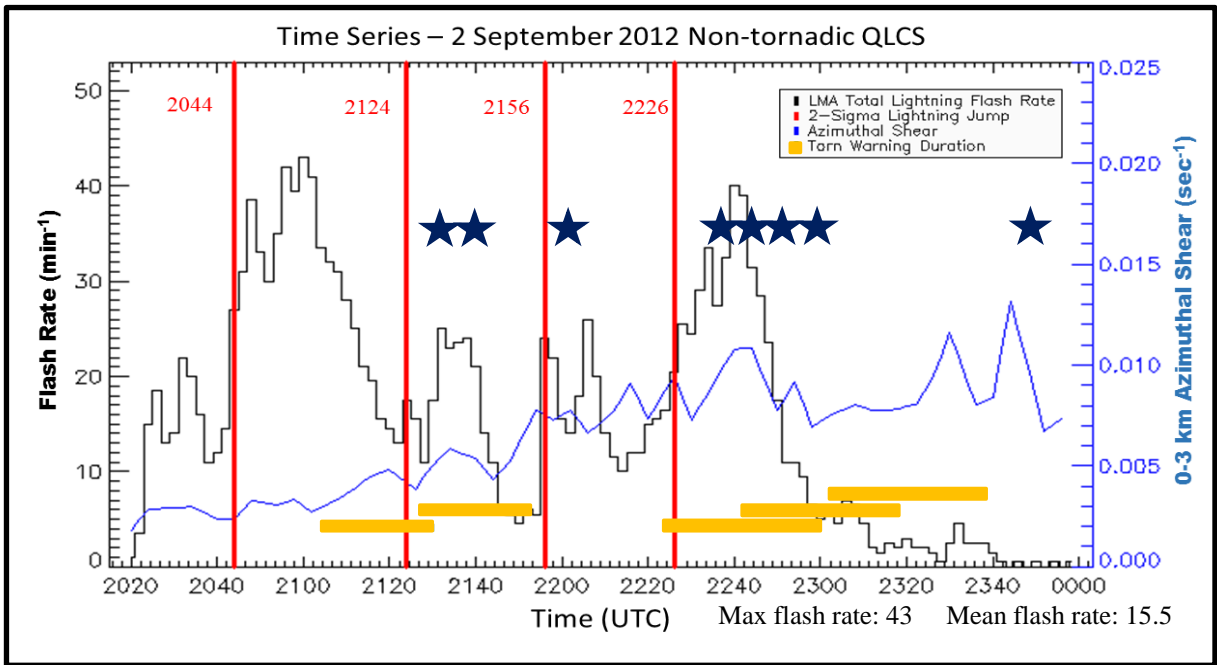


Figure 14: Time series of flash rate [min^{-1}], time of lightning jump, maximum 0-3 km azimuthal shear [sec^{-1}], tornado warning durations and severe wind reports from tracked cell from 2020 UTC to 2355 UTC on 2 September 2012